Title
Quantitative magnetic resonance imaging for chronic liver disease

Journal
British Journal of Radiology, 94(1121)

ISSN
0007-1285

Authors
Cunha, Guilherme Moura
Navin, Patrick J
Fowler, Kathryn J
et al.

Publication Date
2021-05-01

DOI
10.1259/bjr.20201377

Peer reviewed

BJR

https://doi.org/10.1259/bjr.20201377

Received: 25 November 2020 | Revised: 12 February 2021 | Accepted: 18 February 2021

Cite this article as:
Moura Cunha G, Navin PJ, Fowler KJ, Venkatesh SK, Ehman RL, Sirlin CB. Quantitative magnetic resonance imaging for chronic liver disease. *Br J Radiol* 2021; **94**: 20201377.

REVIEW ARTICLE

Quantitative magnetic resonance imaging for chronic liver disease

[1]GUILHERME MOURA CUNHA, MD, [2]PATRICK J NAVIN, [1]KATHRYN J FOWLER, [2]SUDHAKAR K VENKATESH, [2]RICHARD L EHMAN and [1]CLAUDE B SIRLIN

[1]Department of Radiology, Liver Imaging Group, University of California San Diego, San Diego, CA, USA
[2]Department of Radiology, Mayo Clinic, Rochester, MN, USA

Address correspondence to: Dr Guilherme Moura Cunha
E-mail: *gcunha@health.ucsd.edu*

Guilherme Moura Cunha and Patrick J Navin have contributed equally to this study and should be considered as co-first authors.

ABSTRACT

Chronic liver disease (CLD) has rapidly increased in prevalence over the past two decades, resulting in significant morbidity and mortality worldwide. Historically, the clinical gold standard for diagnosis, assessment of severity, and longitudinal monitoring of CLD has been liver biopsy with histological analysis, but this approach has limitations that may make it suboptimal for clinical and research settings. Magnetic resonance (MR)-based biomarkers can overcome the limitations by allowing accurate, precise, and quantitative assessment of key components of CLD without the risk of invasive procedures. This review briefly describes the limitations associated with liver biopsy and the need for non-invasive biomarkers. It then discusses the current state-of-the-art for MRI-based biomarkers of liver iron, fat, and fibrosis, and inflammation.

INTRODUCTION

Chronic liver disease (CLD) causes significant morbidity and mortality, with downstream societal costs. The prevalence of CLD has rapidly increased over the past two decades worldwide, placing CLD among the main causes of premature mortality.[1,2] The most common etiologies of CLD are viral hepatitis and non-alcoholic fatty liver disease (NAFLD).[2,3]

CLD is characterized by distinctive histological abnormalities, which include substance deposition (*e.g.* fat, iron), inflammation, hepatocellular injury, fibrosis, and ultimately vascular and architectural remodeling.[4] Currently, the clinical standard for diagnosing the presence and assessing the severity of CLD is liver biopsy with histology analysis. Liver biopsy suffers from diagnostic limitations and is risky, which makes it less than ideal for screening and monitoring. Hence, validation of accurate and precise non-invasive methods to assess CLD is an area of active research. Leading candidates for this purpose include serum or circulating biomarkers, clinical decision rules, and imaging methods. The imaging methods are further defined by modality: ultrasound, CT, and MRI.[5–8]

This article focuses on MRI-based biomarkers. It begins with a discussion biopsy and the need for non-invasive assessment of CLD, and it then reviews the current state-of-the-art for MRI-based biomarkers of liver iron, fat, fibrosis, and inflammation.

CURRENT ROLE AND LIMITATIONS OF BIOPSY: ARGUMENT FOR NON-INVASIVE BIOMARKERS

In the setting of CLD, liver biopsy plays three roles: diagnosis, assessment of disease severity, and longitudinal monitoring. Although considered the reference standard for each of these three roles, biopsy is prone to sampling-associated error and high inter-reader variability.[4] A study that compared simultaneous intraindividual paired percutaneous liver biopsies for the assessment of NAFLD found that steatosis grades were different in 22% of patients and differed by at least one fibrosis stage in 41% of patients.[9] Additional analysis showed that if only one of the biopsies was considered for diagnosis, steatohepatitis would have been missed in 24% of patients. Multiple factors contribute to liver biopsy variability, including disease spatial heterogeneity, small and inconsistent tissue sample size, and

subjective interpretation with modest intra-reader agreement.[10,11] The semiquantitative nature of histological scoring is an additional limitation. For example, liver steatosis grading is performed by visual estimation of the proportion of hepatocytes containing fat (no steatosis,<5%; Grade 1, 5%–33%; Grade 2, 33–66%; Grade 3 > 66%).[12] These broad brackets of severity complicate statistical analyses in research and limit detectability of small longitudinal changes in liver fat content both clinically and for research. Similarly, semiquantitative scores are used for staging liver fibrosis, which maxes out at cirrhosis (Stage four fibrosis in most scoring systems), effectively grouping the large swath of patients with cirrhosis into a single category. Patients with cirrhosis have a broad biological range of disease, ranging from asymptomatic to severe morbidity and in some cases, deadly complications. To capture this biological range, a quantitative test with a large and continuous dynamic range would be preferable.

Recognizing these limitations, several authors have attempted to automate biopsy analysis using quantitative techniques and deep learning algorithms.[13–15] Further research is needed to determine the clinical advantages of using these methods for biopsy analysis; however, the analysis of a single biopsy, no matter how sophisticated, cannot overcome the limitations of spatial variability and complication risk, major impediments for longitudinal or repeated monitoring. In one large series of 2740 percutaneous liver biopsies, approximately 2.3% resulted in complications, which ranged from mild (*e.g.* transient pain) to severe (*e.g.* bleeding, punctured gallbladder, pneumothorax).[16] Importantly, of the total number of planned biopsies for that study, 429 procedures were withheld due to low platelet count as a contraindication to the biopsy procedure. Considering that low platelet count is relatively common in patients with advanced CLD, a significant proportion of patients are not suitable for biopsy evaluation.

MR-based biomarkers have been widely adopted to overcome the limitations associated with liver biopsy.[17] Due to their non-invasive nature, these methods are safer, while assessing the entire liver which obviate sampling problems. Further, MRI-based biomarkers yield quantitative measurements that have been proven to be accurate and precise for the diagnosis, assessment of severity, and longitudinal monitoring of CLD.

LIVER IRON

Background

Although iron is a vital micronutrient playing a pivotal role in the oxygen transport system of hemoglobin, excessive iron accumulation in the liver leads to oxidative stress, mitochondrial dysfunction and DNA damage, all of which result in hepatocyte injury.[17] Several hepatic and extrahepatic chronic conditions may cause liver iron accumulation – including hereditary hemochromatosis, hematological diseases (*e.g.* thalassemia, sickle cell) and frequent blood transfusions, and primary liver diseases – through a variety of mechanisms as reviewed elsewhere.[18–21] Assessment of liver iron is useful to inform the need for chelation therapies and to monitor treatment response. To date, liver biopsy remains the reference standard for liver iron quantification, which is most often performed semiquantitatively, using a four-point grading scale.[21] Quantitative measurements can be performed using biochemical techniques allowing for objective measurements of liver iron concentration (LIC); determined as the amount of iron in μmol or grams per gram of dry weight liver tissue. In normal individuals, LIC ranges from 3.6 to 36 μmol/g (0.2 to 2 mg g^{-1}) of dry weight. Values higher than 36 up to 150 μmol/g (8.3 mg g^{-1}) are considered mild overload, 150 to 300 μmol/g (16.7 mg g^{-1}) moderate overload, and >300 μmol/g severe iron overload.[18,22]

MRI-based liver iron quantification-Basic concepts

MRI-based methods for liver iron quantification exploit the effect of iron on MRI signal. Iron, a ferromagnetic substance, alters the local magnetic field, accelerates transverse relaxation, and shortens T2 and T2* relaxation time constants. These continuous variables are measured in units of time (milliseconds) and can be converted into relaxivity rates (R2 = 1/T2, R2*=1/T2*, both reported as 1/s). Conversion from relaxation time constants to relaxivity rates is useful as rates are directly related to LIC over a large biologically relevant range. The relationship between R2 and LIC is curvilinear while the relationship between R2* and LIC is linear over a wide biological range (Figure 1). Although iron also accelerates longitudinal relaxation (*i.e.* it shortens T1 time constants and increases R1 relaxivity rates), this effect is weaker and not commonly applied for iron quantification.

Different approaches to estimate LIC using MRI have been proposed, all leveraging the inverse relationship between iron content and signal intensity on T2 or T2*-weighted images. One of the first successful approaches was pioneered by Gandon et al[23]. In this method, signal intensity in liver and in a reference tissue with no iron (paraspinal muscle) are measured on multiple acquisitions with increasing TEs using the body coil. Yet, this approach has limitations including the need for multiple acquisitions, the assumption that the reference tissue has constant signal intensity (which may not be true), and a tendency to overestimate LIC.

Quantitative approaches that do not require a reference tissue for comparison were subsequently developed.[24,25] The so-called R2 relaxometry techniques use spin-echo-based acquisitions with a fixed relaxation time (TR) and increasing TEs to estimate R2 relaxivity values. Pioneered by St. Pierre et al, the leading R2 relaxivity method uses a biexponential model and an external reference phantom to estimate R2 and a non-linear regression algorithm to link R2 with LIC.[24] The algorithm was validated using LIC measured in contemporaneously obtained liver tissue samples[24,25] and subsequently commercialized (FerriScan®) [26]. Disadvantages of the commercial method are its prolonged acquisition time, requirement for an external phantom, and the additional time and cost associated with offline analysis.

Recently, R2* relaxometry has become commonplace in clinical practice with availability of the technology on most MR scanners.[22] The concept is similar to R2 relaxometry methods, relying on MRI signal decay at increasing TEs, but using a GRE sequence. GRE sequences are more sensitive to the presence of iron since signal decay is caused by both T2 and T2* effects. R2*

Figure 1. Conversion from relaxivity to LIC over a large biological range. The relationship between R2 and LIC is curvilinear while the relationship between R2* and LIC is mostly linear. Higher iron is associated with higher relaxivity rates.

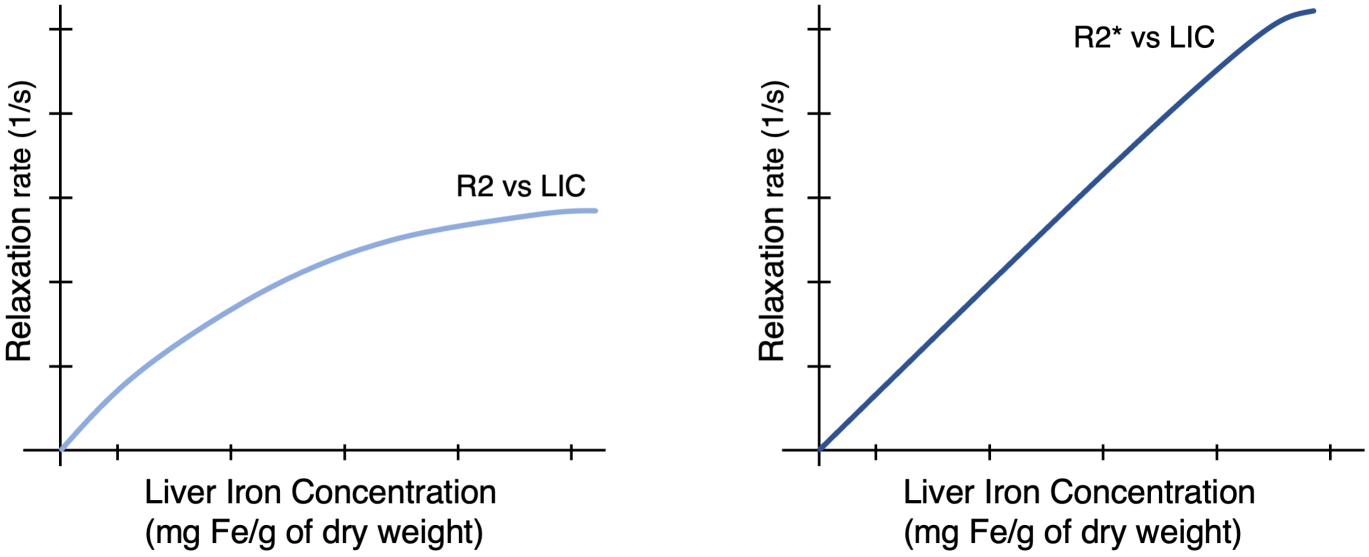

methods have practical advantages: they are fast (can be acquired in a single breath-hold), do not require offline analysis, and, if designed properly, allow for the simultaneous quantification of liver fat (as discussed later). Further, by fitting the data at the voxel level using appropriately spaced echo times, it is possible to produce parametric maps (R2* maps) that are easily interpreted (Figure 2). A few different approaches for measuring R2* have been proposed.[22] To date, these do not perfectly agree mainly because of differences in acquisition parameters and signal modeling.

Clinical and research implementation

The clinical and research implementation of MRI-based liver iron quantification techniques is in evolution, with no single MRI-based method universally accepted. All the above-described proposed methods have advantages and disadvantages. Depending on availability and if applied and interpreted with care, each could be utilized to diagnose patients with iron overload, assess the amount of iron overload, identify patients suitable for clinical trials, inform treatment decisions, and monitor patients longitudinally.

While all three methods might be suitable depending on availability, R2 as measured by Ferriscan® is generally considered the gold standard, and a calibration equation converting R2 to LIC is available in the literature.[25] There is not yet a universally established calibration formula to convert R2* to LIC, with different diagnostic cutoffs published so far. These inconsistencies have challenged the acceptance of R2* methods in clinical care and clinical trials.

Fortunately, recent advances in the field, including the development of more accurate and less-error-prone complex-data based techniques,[27] suggest that in the next few years a standardized method for measuring R2* and a universal conversion for R2* to LIC will be established. We anticipate that those developments will usher widespread acceptance of R2* methods for clinical care and research.

Figure 2. Complex-based R2* maps at 3T. Three different patients with mild, moderate and severe liver iron overload

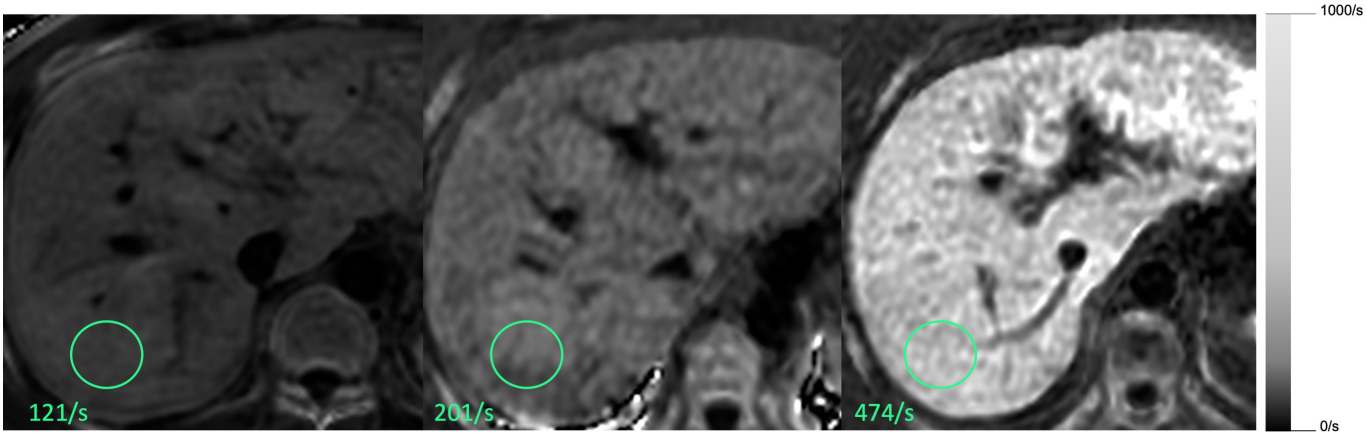

Pitfalls and future directions

The high sensitivity to susceptibility effects of GRE sequences is an advantage (*e.g.* more sensitive to the presence of iron), but also a limitation. It may cause inaccurate results in the presence of other contributors to magnetic field inhomogeneity, such as air or metal, and when liver iron is markedly elevated. Extreme levels of iron may even make R2* estimation impossible due to substantial signal loss earlier than the first signal echo, particularly at 3T.[28] Defining the iron levels beyond which R2* estimation becomes unreliable is an area of active investigation. Further, emerging data suggest that the presence of liver fat might confound R2* measurements,[29] especially in the relatively low iron and high fat range. Two main mechanisms affect R2* estimations in the presence of liver fat: signal intensity oscillation due to fat-water interference and signal intensity decay due to microscopic field inhomogeneities caused by fat droplets. The former mechanism can be addressed through mathematical modeling,[27] while the latter is still to be solved. This correlation between liver fat content and R2* is relevant as patients with NAFLD may be erroneously classified as having excess liver iron.

LIVER FAT

Background

Liver fat accumulation occurs most commonly due to alterations in fat and insulin metabolism, leading to an abnormal buildup of triglycerides within hepatocytes.[30] Accumulation of fat within hepatocytes can also occur secondary to cellular injury. Fatty liver is defined when hepatic steatosis (*i.e.* accumulation of fat within hepatocytes) affects ≥5% hepatocytes.[12] In this section, we will focus on NAFLD, in which fat accumulates in the absence of significant alcohol ingestion. NAFLD has a variable disease course, from non- or slowly progressive isolated steatosis (non-alcoholic fatty liver, NAFL) to its more rapidly progressive form (non-alcoholic steatohepatitis, NASH).[30] While the exact relationship between the amount of liver fat and progressive forms of NAFLD is not established, the quantification of liver fat is recognized as an important clinical biomarker to assess disease status and as a marker of response to antisteatogenic drugs.[31]

MR-based liver fat quantification -Basic concepts

The key concept of MR-based methods is that liver fat can be quantified by decomposing the MR signal into fat and water components. Historically, MR spectroscopy (MRS), a non-anatomical method of measuring MR signal in a prescribed volume was considered the gold standard due to its accuracy in quantifying lipid relative to water in biological tissues. Although MRS- and MRI-based techniques share some physics concepts, adequate MRS data can be technically challenging to acquire, may require an expert spectroscopist for analysis and interpretation, and may also suffer from sampling variability.[32,33] By comparison, MRI-based methods are easier to implement and interpret and allow whole-liver coverage; hence, these methods are more commonly used in clinical practice and research. Signal fat fraction, that is, the MR signal attributed to fat, can be measured using fat-suppressed techniques or chemical shift-based techniques. The former separates the MR signal by subtracting a pair of magnitude images acquired with and without fat saturation. As complete and homogeneous fat signal saturation is virtually impossible with *in-vivo* imaging, this technique is unreliable and rarely used for fat quantification. The latter, chemical shift-based techniques, is the scope of this review and separate the water and fat signal components by acquiring GRE images at appropriately spaced TEs for this purpose. Measurements can be performed using only magnitude data (magnitude-based approach) or both magnitude and phase information (complex-based approach). Advanced variants of these methods address factors that confound the fat signal, including the spectral complexity of fat, T1 bias, T2* signal decay, noise bias, and phase errors such as those caused by eddy currents.[33] When these confounding factors are addressed, the proton density fat fraction (PDFF) is measured.

PDFF is an inherent tissue property and reflects the proportion of mobile protons attributable to fat over the total proton density in a given tissue. MRI-PDFF is independent of field strength and scanner platform, and accurately correlates with histology determined liver triglyceride concentration.[17] Pixel-based measurements can be made to produce parametric PDFF maps that are easy to interpret while displaying the spatial distribution of liver fat (Figures 3 and 4).

Figure 3. Magnitude-based PDFF maps. Three different patients with mild, moderate and severe liver steatosis.

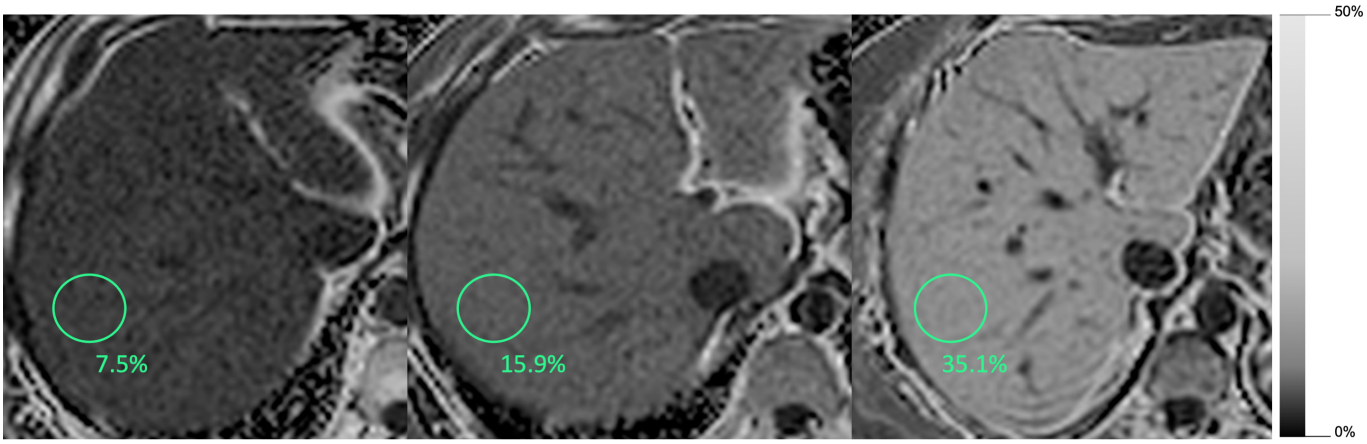

Figure 4. 46-year-old female, magnitude-based PDFF maps. Segmental distribution of liver fat is displayed. Segment I has lower fat fraction compared to other liver segments.

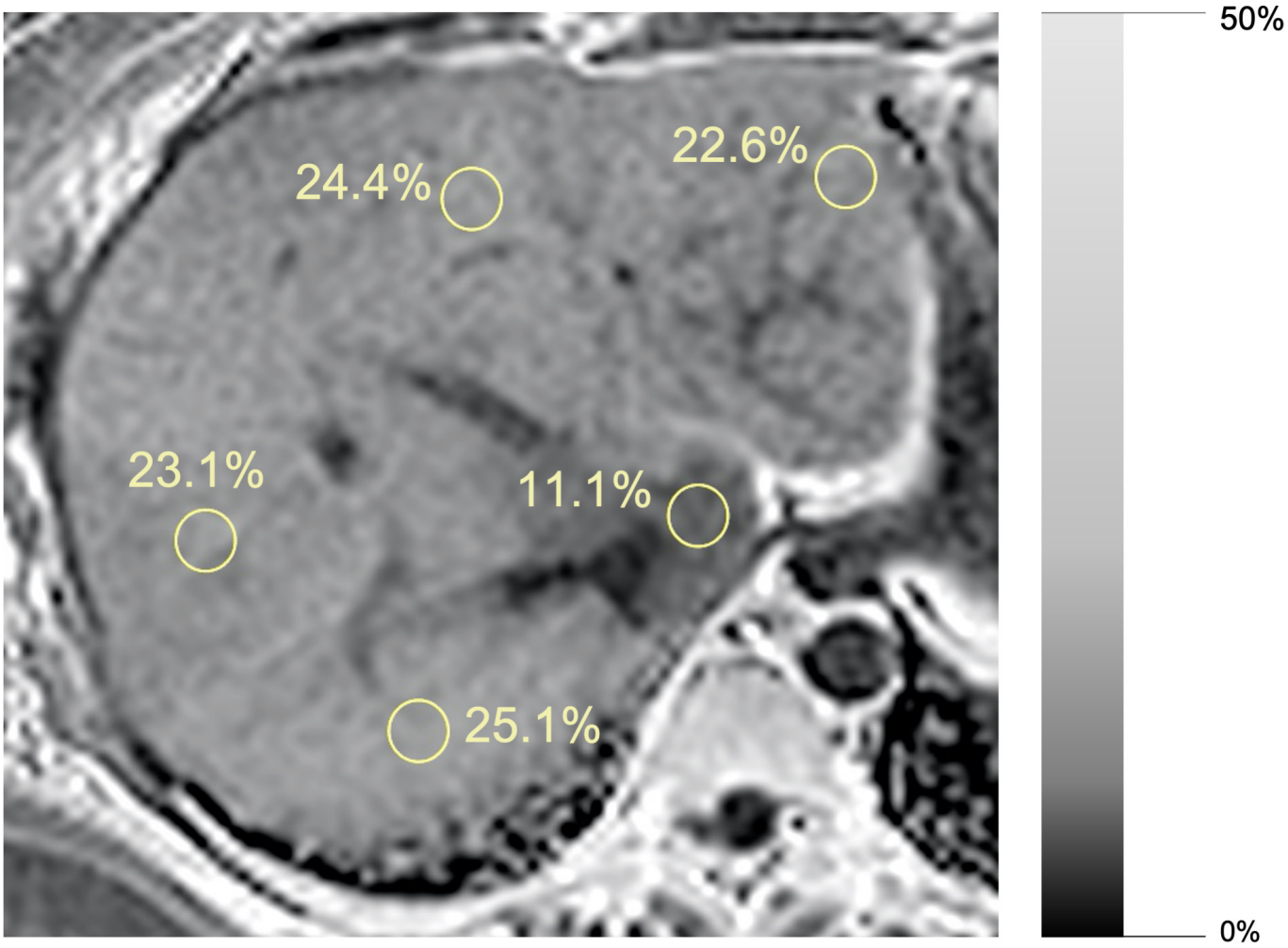

Clinical and research implementation

Commercially available chemical-shift-based methods can provide whole liver coverage in a single breath-hold and can generate PDFF maps of the entire liver. These methods can be performed before or after administration of contrast agents, which do not impact the results. Since the methods measure and correct for R2* effects, they also generate R2* maps, permitting simultaneous assessment of liver iron.[33] Images are analyzed by placing regions of interest (ROIs) in representative portions of the liver and recording the mean PDFF and R2* values from the ROIs.

Although PDFF correlates closely to triglycerides concentration, these are not equivalent, as a small proportion of triglycerides in biologic tissues is invisible to MRI.[34] Similarly, although histology determined steatosis and PDFF are expressed as percentages, these refer to different measurements (the former reflects the percentage of cells containing intracellular fat droplets, while the latter refers to the fat fraction of a given volume). Hence, the relationships between PDFF and steatosis grades are non-linear. Different PDFF cut-offs have been proposed to classify steatosis grades,[35–37] with high-specificity cutoffs of about ≥5.2%, ≥16.3%, and ≥21.7% corresponding to steatosis grades of ≥1, ≥2, and 3, respectively.[38] Studies have also investigated the accuracy and reproducibility of MRI-PDFF in different settings and populations.[37–43] Two metanalysis, showed high accuracy, reproducibility, and repeatability of MRI-PDFF for the assessment of steatosis across different field strengths, vendors, and reconstruction methods.[38,42]

Due to its non-invasive nature, accuracy, and high reproducibility, MRI-PDFF has emerged as the preferred method for non-invasive liver fat quantification in clinical and research settings[17] and is now used as an endpoint in antisteatotic phase two clinical trials.[31–43] *A* ≥ 30% relative reduction in PDFF has been proposed as non-invasive indicator of treatment response in NASH clinical trials.[44] Recent studies suggest that higher PDFF is a risk factor for fibrosis progression in untreated patients and that PDFF is more sensitive than liver biopsy in detecting changes in liver fat content in clinical trials.[43,44]

Pitfalls and future directions

Some limitations of MRI-PDFF merit mention. At the low fat-fraction range, liver PDFF estimation can be inaccurate due to

the confounding effect of background signal noise. In patients with severe liver iron overload, PDFF estimation may be impossible because rapid signal loss from dephasing obscures fat-water signal oscillation. The level of R2* beyond which PDFF estimation becomes unreliable is not yet known, however. To date, the commercially available sequences have low spatial resolution and are prone to imaging artifacts, which limit their ability to detect or characterize fat in small liver lesions. Emerging advancements include faster image acquisition, free-breathing protocols to improve patient comfort, and deep-learning (DL)- based automated analysis.[45]

LIVER FIBROSIS

Background

Liver fibrosis is a response to repetitive cellular injury. Hepatocyte damage and associated inflammatory response lead to the activation of stellate cells, proliferation of fibroblasts/myofibroblasts, and excessive extracellular matrix collagen deposition. The diagnosis and assessment of hepatic fibrosis is classically performed on histological analysis. The severity of fibrosis is scored as stages, typically five in most histological scoring systems. The stage of fibrosis is an important prognostic marker. It demonstrates a strong positive correlation to all-cause mortality, liver-related mortality, decompensation of liver disease and liver-disease complications.[46,47]

Given the limitations of liver biopsy previously outlined, considerable research has been directed at developing reliable non-invasive biomarkers for assessing liver fibrosis, with MRI-based biomarkers emerging as practical tools for this purpose.

The presence of hepatic fibrosis generally causes little anatomic change in the liver until late in the disease. Therefore, conventional anatomic imaging with MRI or other modalities has low sensitivity for detecting fibrosis and cannot be used to reliably assess severity.[48] Investigators have focused on exploring multiple MRI-based quantitative and semiquantitative biomarkers. Studies have demonstrated that all of these tissue biomarkers have some relationship with liver fibrosis. Recently, DL- and radiomics-based methods have attempted to provide models to best predict the presence of fibrosis with promising results.[49,50] However, among these technologies, magnetic resonance elastography (MRE) has emerged over the last decade a leading non-invasive and quantitative method for detecting and staging liver fibrosis.[48]

MR elastography–Basic concepts

Tissue stiffness is a qualitative term used to describe the ability of tissues to resist deformation from external or internal forces. The term "stiffness" is often used interchangeably with the more formal terms, shear elasticity and shear modulus.[51] MRE measures stiffness of tissues with the results expressed as the magnitude of the complex shear modulus in units of kilopascals (kPa).

A flat plastic drum-like device is fastened against the right lower anterior chest wall over liver using an elastic strap. This device applies low-amplitude vibrations (typically at 60 Hz), which generate propagating shear waves with amplitudes in the range of tens of microns.[52] A modified phase-contrast pulse sequence with cyclic motion encoding gradients is used to image the pattern of shear wave propagation in the liver. The MRI scanner automatically processes the acquired wave images to generate "elastograms" (Figure 5), which depict the spatial distribution of stiffness in each slice. The system also calculates a "confidence map", which excludes the pixels with unreliable stiffness values.

Clinical and research implementation

MRE requires approximately one minute of acquisition time (between one and four breath-holds of about 15 s) and can be included in a standard MRI exam of the liver. Typically four slices are obtained through the widest portion of the liver. MRE

Figure 5. Contrast-enhanced portal venous phase images and correlating color coded elastogram of five different subjects with METAVIR fibrosis stages F0 to F4 confirmed on histopathological analysis.

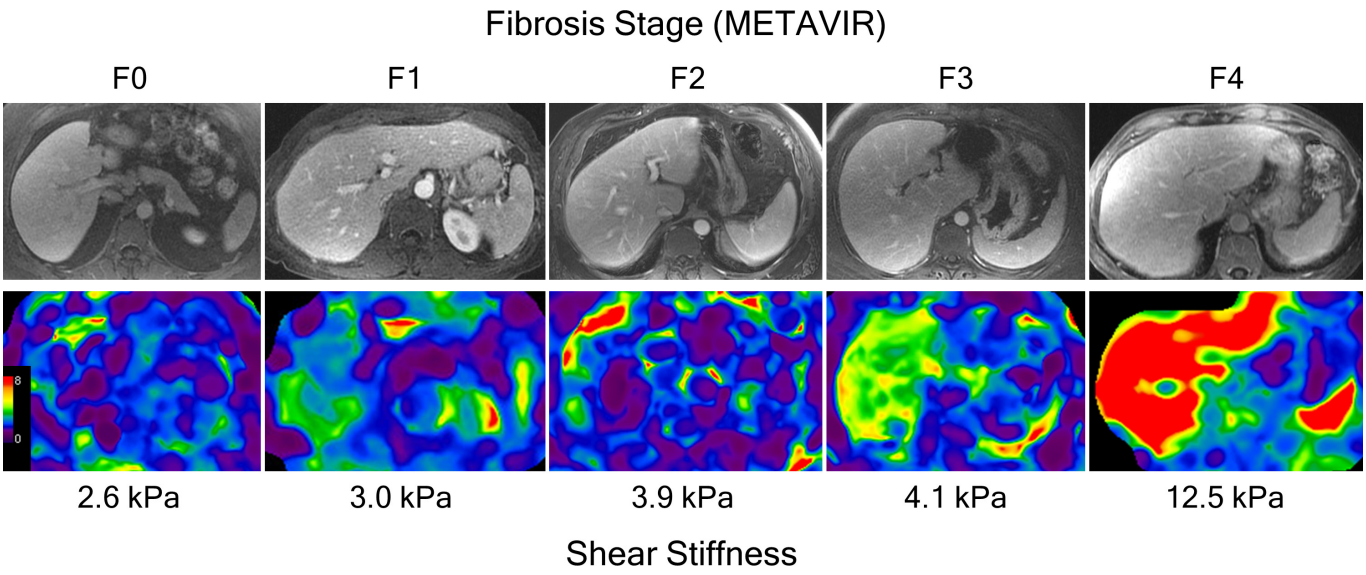

exams are analyzed by drawing regions of interest (ROIs) over the liver on elastograms and recording mean stiffness values. A standardized approach for manual ROI placement is described in the "consensus profile" for "MR Elastography of the Liver", published by the RSNA Quantitative Biomarkers Alliance (QIBA) in 2018.[53] In the research setting, some investigators have proposed automated methods for analysis.[54]

MRE is now considered the most accurate non-invasive technique for detecting and staging liver fibrosis.[55] Using histological analysis as gold standard, MRE-stiffness cut-offs of 2.7–2.9 kPa, 3.3–3.5 kPa, and 3.8–3.9 kPa have been proposed for detecting any fibrosis, fibrosis stage ≥2, and fibrosis stage ≥3, respectively.[56–58] The exact cut-offs, however, depend on the underlying etiology of CLD and the prevalence and burden of fibrosis in the study population.[51] A number of systematic reviews have demonstrated the validity of MRE in classifying the stage of fibrosis.[58–61] In a systematic review of 12 studies, the area under the receiver operating characteristic curve (AUROC) of MRE was 0.84 for diagnosing stage ≥1, 0.88 for diagnosing stage ≥2, 0.93 for diagnosing stage ≥3 and 0.92 for diagnosing cirrhosis, with sensitivities of 80–98%, specificities of 90–100% and accuracies of 89–99%, depending on the fibrosis classification of interest.[59]

An important metric for any quantitative imaging technology is test-retest repeatability, which expresses how well the technology can detect a biological change. The QIBA MRE Consensus Profile, based on an update of a meta-analysis of test-retest studies, has stated that a change of at least 19% in liver stiffness, measured with the same equipment, is likely to represent a true biological change.[53] MRE also benefits from excellent intra- and inter-observer reliability, with stiffness values reproducible on multiple platforms.[62]

In addition to staging fibrosis, MRE might be useful for risk stratification. Some studies have shown that baseline hepatic stiffness predicts future risk of cirrhosis development in NAFLD,[63] clinical decompensation in cirrhotic patients[64] or HCC development and recurrence.[65] The utility and cost-effectiveness of applying baseline MRE for these purposes have not yet been established, however.

Longitudinal monitoring of patients with CLD is often required to identify those at risk of developing complications. In a prospective study on patients with NAFLD, a 15% increase in MRE values was associated with histological fibrosis progression on biopsy.[66] Interval changes in liver stiffness measured with MRE can also predict risk of hepatic decompensation.[67] While further validation is needed, these emerging results suggest that MRE might be useful for monitoring patients longitudinally and could potentially be used to assess treatment response in clinical trials.

Finally, MRE shows promise for identifying mimics of hepatic fibrosis such as nodular regenerative hyperplasia and for differentiating cirrhotic and non-cirrhotic causes of portal hypertension[68] (Figure 6).

Pitfalls and future directions

Failure of MRE is rare, quoted as 4.3% in a meta-analysis of 12 studies.[59] In the past, the most common cause of technical failure in hepatic MRE was the presence of excess iron in liver parenchyma. Early versions of MRE used a GRE sequence, which is sensitive to signal loss from the presence of elevated liver iron. This problem was more apparent in 3.0T imagers than in 1.5T systems. The introduction of spin-echo echo planar (SE EPI) MRE sequences, which are less sensitive to liver iron overload, has ameliorated the problem and reduced the technical failure rate to 2%.[69] Most remaining failures are due to improper placement of the driver device or failure to ensure coupling with the body. These errors can be recognized by properly trained MR operators and in most cases, the problem can be addressed and the acquisition completed promptly.

Current commercially available MRE technology uses a two-dimensional wave propagation model for acquisition and processing to simplify the implementation and accelerate acquisition. While the validity of liver stiffness measurements obtained with this approach has been established in clinical practice and research, the model is subject to error if a significant component of wave is oblique to the acquired transverse imaging planes. More advanced versions of MRE technology acquire and process three-dimensional wavefield data, promising to provide more accurate measurements of stiffness throughout the liver with increased measurement repeatability and reproducibility.[70] Newly introduced flexible drivers enhance patient comfort and may improve shear wave illumination of the liver, while introduction of automated methods for MRE analysis can improve workflow and measurement reproducibility.[54,71]

LIVER INFLAMMATION

Background

Hepatic fibrosis and cirrhosis are considered as the end point of liver disease. Inflammation from a range of etiologies, dictate the rate and severity of fibrotic change and so reflect the grade of disease activity.[12] As with other components of CLD, histology is considered the gold standard for assessment. In addition to the previously mentioned limitations of biopsy, a limitation specific to the evaluation of inflammation is that histopathology only assesses the cellular components of inflammation and cannot assess other important components such as edema and hyperemia.

MRI biomarkers for assessing inflammation

DWI can assess the random motion of water molecules (diffusion), which is thought to be altered in inflamed hepatic tissue. Apparent diffusion coefficient (ADC), a marker of diffusion, demonstrated promising results in early studies assessing inflammation from varying etiologies, although subsequent studies reported contradictory findings.[72–76] One problem with using ADC is that it is affected by perfusion in addition to diffusion effects, and the two effects may offset or confound each other. Intravoxel incoherent motion (IVIM) is a more advanced method of analyzing the diffusion signal that can estimate diffusion and perfusion effects separately. In principle, perfusion-related parameters such as the perfusion fraction and pseudodiffusion

Figure 6. An example of MRE as a problem-solving tool. Contrast-enhanced portal venous phase of two separate 30-year-old male patients with abnormal liver function tests (*A* + B). Morphological changes suggest advanced fibrosis or cirrhosis with portal hypertension in both patients. c: Color-coded elastogram demonstrates only minimally increased liver stiffness. Biopsy demonstrates diffuse nodular regenerative hyperplasia without significant fibrosis. d: Color-coded elastogram demonstrates markedly increased liver stiffness consistent with stage four fibrosis (cirrhosis), which was confirmed on biopsy.

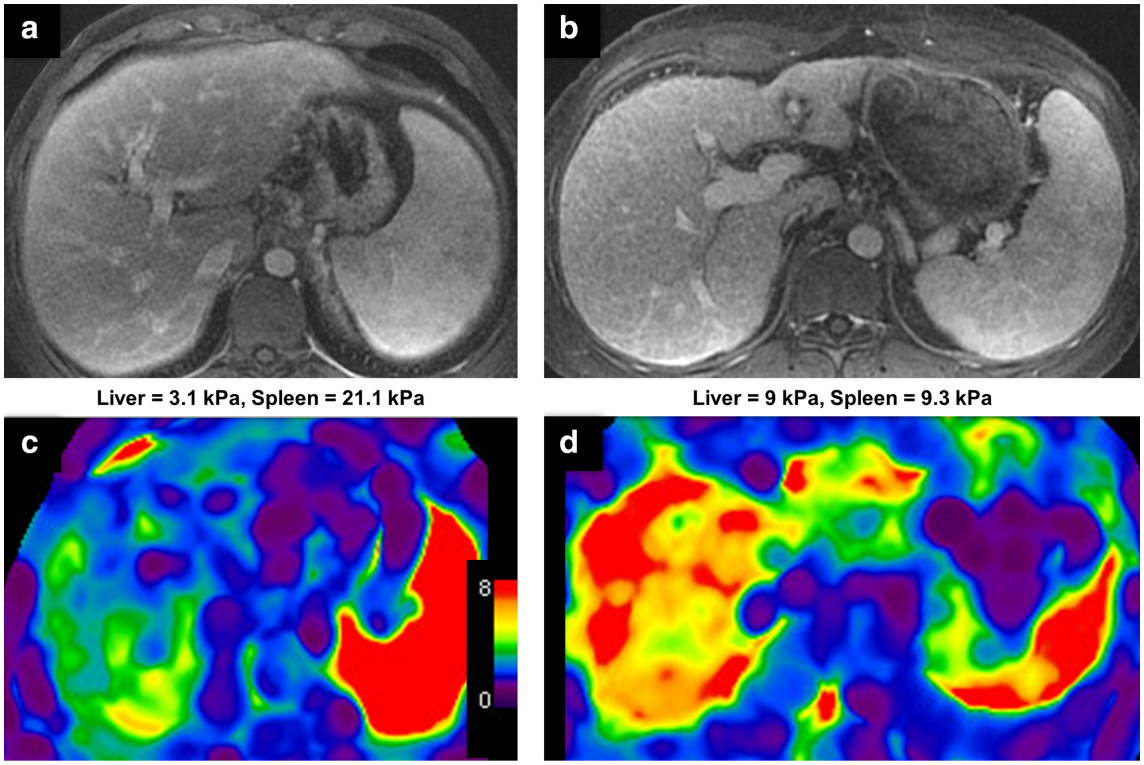

coefficient might reflect microvascular alterations associated with inflammation. The capability of these parameters to detect inflammation non-invasively is limited, with multiple *in-vivo* studies showing only minimal to no correlation with inflammation.[73,75,77] A recent study, however, did demonstrate a stronger correlation for the perfusion fraction.[78]

Dynamic contrast-enhanced perfusion imaging is another method for assessing perfusion non-invasively. This method measures the signal in liver, portal vein, and other structures before and at multiple time points after injection of a contrast agent. By applying sophisticated tissue compartment models, the arterial and portal perfusion to the liver can be estimated. The association of contrast-enhanced MRI perfusion parameters to hepatic inflammation has been weak, perhaps due to overlapping effects of inflammation and other physiological and structural changes associated with CLD.[79] A single study did, however, demonstrate the potential of the arterial fraction parameter in distinguishing mild activity from moderate-to-severe activity and for differentiating no activity from mild activity.[79]

Other investigators have explored the relaxation parameters T1, T1ρ, and T2 for assessing hepatic inflammation, with modest success.[80–82] A proprietary technique involving calculation of a corrected T1 relaxation time has shown promise as a biomarker for liver inflammation and cell injury.[83] Further, the development of DL-based models and the advent of radiomics may improve the ability to assess inflammation. In a recent retrospective study, a radiomics model based on a T2W sequence showed encouraging results for detecting hepatic inflammation.[84]

The use of 3D MRE with different inversion models has introduced the potential to isolate an inflammatory process from fibrotic change (Figure 7). Hepatic stiffness measured with MRE derives from a static component (elasticity) and dynamic component (viscosity or loss modulus). The dynamic component is thought to be affected by inflammation. Two 3D MRE-derived parameters, the damping ratio and shear loss modulus, have demonstrated encouraging signs in animal models.[85] In a cohort of 175 bariatric surgery candidates, 81 with histological NASH, a multivariable model involving the damping ratio, shear stiffness and PDFF provided an AUC of 0.73 for diagnosing NASH.[86] Changes in these parameters were also found to correlate with a resolution of NASH following bariatric surgery.[87]

Clinical and research implication– Towards the non-invasive diagnosis of NASH

Clinically, the differentiation of hepatic inflammation from normal hepatic parenchyma and fibrotic tissue is particularly relevant in the management of NAFLD. Since the presence of NASH portends high risk for progressing to end-stage liver disease,[88] the identification of patients with NASH is important to trigger more intense intervention and close follow-up.

Figure 7. Select images of 3D MRE and chemical-shift MRI-derived PDFF on subjects with NAFLD. The subject in the top row has biopsy-proven NASH and stage three fibrosis. The subject in the bottom row has NAFL without NASH and fibrosis. Note the elevated liver stiffness and decreased damping ratio in the liver in the subject with NASH.

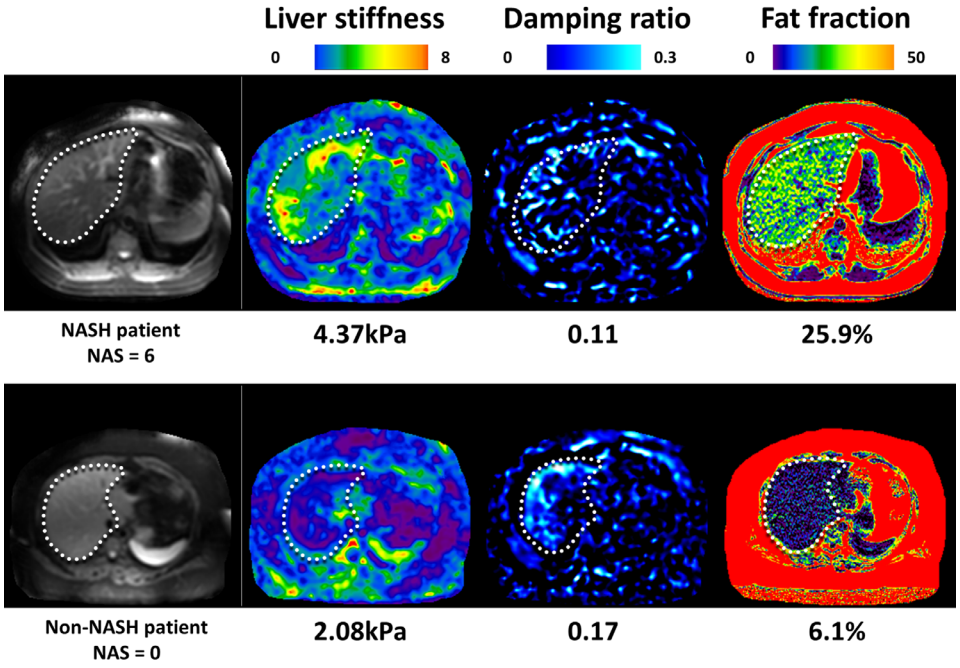

Histologically, NASH is diagnosed when hepatic steatosis is observed with hepatocyte ballooning and lobular inflammation with other additional histological findings. The NAFLD activity score (NAS) is used to grade disease activity in NAFLD.[12] This is an aggregate score based on the grade of steatosis (0–3), lobular inflammation (0–3), and hepatocellular ballooning (0–2). Scores of 5–8 are sometimes considered diagnostic of NASH.

Multiple MRI biomarkers are being explored to specifically distinguish NASH from NAFL. The use of IVIM has produced mixed results from two separate studies.[89,90] The Liver Inflammation and Fibrosis (LIF) score derived from multiparametric T1 and T2* mapping demonstrated an AUROC of 0.80 in diagnosing NASH.[83] MRE using shear stiffness and loss modulus demonstrated correlation with lobular and portal inflammation and excellent diagnostic accuracy in predicting NAS in animal models.[91] A model containing MRE parameters and PDFF can also predict NASH with good diagnostic performance in candidates awaiting bariatric surgery as well as the resolution of NASH following surgery.[86,87]

Cost considerations

The charges for performing and interpreting diagnostic medical procedures vary globally, although there is some consistency in the costs of these tests relative to each other. In the U.S., the "resource-based relative value scale" is a standard method used to guide payments for medical procedures. For diagnostic tests, this method takes into account the costs of purchasing and maintaining equipment, performing the procedure, and interpretating and reporting the results. According to the current schedule of the U.S. Centers for Medicare and Medicaide Services (CMS), the cost of an abdominal MRI exam, which could include PDFF, T2*, and MRE to assess liver fat, iron, and fibrosis, respectively, is $476. An MRI exam consisting only of MRE has a listed charge of $284. For comparison, the CMS reimbursement for Vibration Controlled Transient Elastography (VCTE) is approximately $150 and the charge for liver biopsy and histologic examination is at least $2000. The costs between tests relative to each other in the U.K. are similar. A recent publication listed the unit cost of liver MRI at £101, VCTE at £43, a panel of routine blood tests for CLD at £68, and liver biopsy at £643.[92]

Further, the cost-effectiveness of non-invasive methods for assessing CLD need to be considered in the context of the disease in question. In chronic hepatitis-C infection, modeling studies have suggested that the most cost-effective approach is to treat all patients with any degree of liver fibrosis[93]; in this context, the main value of biomarkers may be for assessing treatment response rather than guiding treatment decisions. In NAFLD, by comparison, modeling studies support the use of non-invasive biomarkers as a cost-effective strategy to stratify risk and direct management decisions. To that end, accurate methods such as MRE are particularly attractive as they confidently exclude advanced liver disease and thereby reduce unnecessary referrals and procedures in patients with only mild disease.[94,95]

CONCLUSION

As we move toward a more personalized approach to patient care, objective biomarkers are required to standardize the grading of CLD and offer accurate prognostic information. Given the limitations of biopsy, non-invasive MR-based biomarkers provide exciting opportunities with minimal risk. Examples such as PDFF and shear stiffness from MRE provide us with robust, reproducible measures to assess liver fat and fibrosis respectively,

which can rival histological accuracy. Additionally, several MRI-based approaches for iron assessment have been developed, and it is anticipated that a standardized approach will be established in coming years. Finally, despite limitations, emerging techniques for the assessment of inflammation and diagnosis of NASH demonstrate potential for future use.

REFERENCES

1. Udompap P, Kim D, Kim WR. Current and future burden of chronic nonmalignant liver disease. *Clin Gastroenterol Hepatol* 2015; **13**: 2031–41. doi: https://doi.org/10.1016/j.cgh.2015.08.015
2. Stepanova M, De Avila L, Afendy M, Younossi I, Pham H, Cable R, et al. Direct and Indirect Economic Burden of Chronic Liver Disease in the United States. *Clin Gastroenterol Hepatol* 2017; **15**: 759–66. doi: https://doi.org/10.1016/j.cgh.2016.07.020
3. Younossi ZM, Stepanova M, Afendy M, Fang Y, Younossi Y, Mir H, et al. Changes in the prevalence of the most common causes of chronic liver diseases in the United States from 1988 to 2008. *Clin Gastroenterol Hepatol* 2011; **9**: 524–30. doi: https://doi.org/10.1016/j.cgh.2011.03.020
4. Goodman ZD. Grading and staging systems for inflammation and fibrosis in chronic liver diseases. *J Hepatol* 2007; **47**: 598–607. doi: https://doi.org/10.1016/j.jhep.2007.07.006
5. Tan Y-W, Zhou X-B, Ye Y, He C, Ge G-H. Diagnostic value of FIB-4, aspartate aminotransferase-to-platelet ratio index and liver stiffness measurement in hepatitis B virus-infected patients with persistently normal alanine aminotransferase. *World J Gastroenterol* 2017; **23**: 5746: 5746: . doi: https://doi.org/10.3748/wjg.v23.i31.5746
6. Wu S, Yang Z, Zhou J, Zeng N, He Z, Zhan S, et al. Systematic review: diagnostic accuracy of non-invasive tests for staging liver fibrosis in autoimmune hepatitis. *Hepatol Int* 2019; **13**: 91–101. doi: https://doi.org/10.1007/s12072-018-9907-5
7. Kramer H, Pickhardt PJ, Kliewer MA, Hernando D, Chen G-H, Zagzebski JA, et al. Accuracy of liver fat quantification with advanced CT, MRI, and ultrasound techniques: prospective comparison with MR spectroscopy. *AJR Am J Roentgenol* 2017; **208**: 92–100. doi: https://doi.org/10.2214/AJR.16.16565
8. Li J, Liu H, Zhang C, Yang S, Wang Y, Chen W, et al. Native T1 mapping compared to ultrasound elastography for staging and monitoring liver fibrosis: an animal study of repeatability, reproducibility, and accuracy. *Eur Radiol* 2020; **30**: 337–45. doi: https://doi.org/10.1007/s00330-019-06335-0
9. Ratziu V, Charlotte F, Heurtier A, Gombert S, Giral P, Bruckert E, et al. Sampling variability of liver biopsy in nonalcoholic fatty liver disease. *Gastroenterology* 2005; **128**: 1898–906. doi: https://doi.org/10.1053/j.gastro.2005.03.084
10. Bedossa P, Dargère D, Paradis V. Sampling variability of liver fibrosis in chronic hepatitis C. *Hepatology* 2003; **38**: 1449–57. doi: https://doi.org/10.1016/j.hep.2003.09.022
11. Davison BA, Harrison SA, Cotter G, Alkhouri N, Sanyal A, Edwards C, et al. Suboptimal reliability of liver biopsy evaluation has implications for randomized clinical trials. *J Hepatol* 2020; **73**: 1322–32. doi: https://doi.org/10.1016/j.jhep.2020.06.025
12. Kleiner DE, Brunt EM, Van Natta M, Behling C, Contos MJ, Cummings OW, et al. Design and validation of a histological scoring system for nonalcoholic fatty liver disease. *Hepatology* 2005; **41**: 1313–21. doi: https://doi.org/10.1002/hep.20701
13. Nasr P, Forsgren MF, Ignatova S, Dahlström N, Cedersund G, Leinhard OD, et al. Using a 3% proton density fat fraction as a cut-off value increases sensitivity of detection of hepatic steatosis, based on results from histopathology analysis. *Gastroenterology* 2017; **153**: 53–5. doi: https://doi.org/10.1053/j.gastro.2017.03.005
14. Homeyer A, Nasr P, Engel C, Kechagias S, Lundberg P, Ekstedt M, et al. Automated quantification of steatosis: agreement with stereological point counting. *Diagn Pathol* 2017; **12**: 80. doi: https://doi.org/10.1186/s13000-017-0671-y
15. Roy M, Wang F, Vo H, Teng D, Teodoro G, Farris AB, et al. Deep-learning-based accurate hepatic steatosis quantification for histological assessment of liver biopsies. *Lab Invest* 2020; **100**: 1367–83. doi: https://doi.org/10.1038/s41374-020-0463-y
16. Seeff LB, Everson GT, Morgan TR, Curto TM, Lee WM, Ghany MG, et al. Complication rate of percutaneous liver biopsies among persons with advanced chronic liver disease in the HALT-C trial. *Clin Gastroenterol Hepatol* 2010; **8**: 877–83. doi: https://doi.org/10.1016/j.cgh.2010.03.025
17. Reeder SB, Hu HH, Sirlin CB. Proton density fat-fraction: a standardized MR-based biomarker of tissue fat concentration. *J Magn Reson Imaging* 2012; **36**: 1011. doi: https://doi.org/10.1002/jmri.23741
18. Deugnier Y, Turlin B. Pathology of hepatic iron overload. *World J Gastroenterol* 2007; **13**: 4755. doi: https://doi.org/10.3748/wjg.v13.i35.4755
19. Nelson JE, Wilson L, Brunt EM, Yeh MM, Kleiner DE, Unalp-Arida A, et al. Relationship between the pattern of hepatic iron deposition and histological severity in nonalcoholic fatty liver disease. *Hepatology* 2011; **53**: 448–57. doi: https://doi.org/10.1002/hep.24038
20. Girelli D, Nemeth E, Swinkels DW. Hepcidin in the diagnosis of iron disorders. *Blood* 2016; **127**: 2809–13. doi: https://doi.org/10.1182/blood-2015-12-639112
21. Brunt EM, Olynyk JK, Britton RS, Janney CG, Di Bisceglie AM, Bacon BR. Histological evaluation of iron in liver biopsies: relationship to HFE mutations. *Am J Gastroenterol* 2000; **95**: 1788–93. doi: https://doi.org/10.1111/j.1572-0241.2000.02175.x
22. Sirlin CB, Reeder SB. Magnetic resonance imaging quantification of liver iron. *Magn Reson Imaging Clin N Am* 2010; **18**: 359–81. doi: https://doi.org/10.1016/j.mric.2010.08.014
23. Gandon Y, Olivié D, Guyader D, Aubé C, Oberti F, Sebille V, et al. Non-Invasive assessment of hepatic iron stores by MRI. *Lancet* 2004; **363**: 357–62. doi: https://doi.org/10.1016/S0140-6736(04)15436-6
24. St Pierre TG, Clark PR, Chua-anusorn W, Fleming AJ, Jeffrey GP, Olynyk JK, et al. Noninvasive measurement and imaging of liver iron concentrations using proton magnetic resonance. *Blood* 2005; **105**: 855–61. doi: https://doi.org/10.1182/blood-2004-01-0177
25. Jhaveri KS, Kannengiesser SAR, Ward R, Kuo K, Sussman MS. Prospective evaluation of an R2* method for assessing liver iron concentration (LIC) against FerriScan: derivation of the calibration curve and characterization of the nature and source of uncertainty in the relationship. *J Magn Reson Imaging* 2019; **49**: 1467–74. doi: https://doi.org/10.1002/jmri.26313
26. Resonance Health. Ferriscan® – MRI measurement of liver iron concentration. 2018. Available from: https://www.resonancehealth.com/products/

ferriscan-mri-measurement-of-liver-iron-concentration.html.
27. Hernando D, Kühn J-P, Mensel B, Völzke H, Puls R, Hosten N, et al. R2* estimation using "in-phase" echoes in the presence of fat: the effects of complex spectrum of fat. *J Magn Reson Imaging* 2013; **37**: 717–26. doi: https://doi.org/10.1002/jmri.23851
28. Doyle EK, Toy K, Valdez B, Chia JM, Coates T, Wood JC. Ultra-Short echo time images quantify high liver iron. *Magn Reson Med* 2018; **79**: 1579–85. doi: https://doi.org/10.1002/mrm.26791
29. Karlsson M, Ekstedt M, Dahlström N, Forsgren MF, Ignatova S, Norén B, et al. Liver R2* is affected by both iron and fat: a dual biopsy-validated study of chronic liver disease. *J Magn Reson Imaging* 2019; **50**: 325–33. doi: https://doi.org/10.1002/jmri.26601
30. Lonardo A, Nascimbeni F, Maurantonio M, Marrazzo A, Rinaldi L, Adinolfi LE. Nonalcoholic fatty liver disease: evolving paradigms. *World J Gastroenterol* 2017; **23**: 6571. doi: https://doi.org/10.3748/wjg.v23.i36.6571
31. Noureddin M, Lam J, Peterson MR, Middleton M, Hamilton G, Le T-A, et al. Utility of magnetic resonance imaging versus histology for quantifying changes in liver fat in nonalcoholic fatty liver disease trials. *Hepatology* 2013; **58**: 1930–40. doi: https://doi.org/10.1002/hep.26455
32. Idilman IS, Keskin O, Celik A, Savas B, Elhan AH, Idilman R, et al. A comparison of liver fat content as determined by magnetic resonance imaging-proton density fat fraction and MRS versus liver histology in non-alcoholic fatty liver disease. *Acta Radiol* 2016; **57**: 271–8. doi: https://doi.org/10.1177/0284185115580488
33. Reeder SB, Cruite I, Hamilton G, Sirlin CB. Quantitative assessment of liver fat with magnetic resonance imaging and spectroscopy. *J Magn Reson Imaging* 2011; **34**: 729–49. doi: https://doi.org/10.1002/jmri.22775
34. Hong CW, Mamidipalli A, Hooker JC, Hamilton G, Wolfson T, Chen DH, et al. Mri proton density fat fraction is robust across the biologically plausible range of triglyceride spectra in adults with nonalcoholic steatohepatitis. *J Magn Reson Imaging* 2018; **47**: 995–1002. doi: https://doi.org/10.1002/jmri.25845
35. Tang A, Desai A, Hamilton G, Wolfson T, Gamst A, Lam J, et al. Accuracy of MR imaging-estimated proton density fat fraction for classification of dichotomized histologic steatosis grades in nonalcoholic fatty liver disease. *Radiology* 2015; **274**: 416–25. doi: https://doi.org/10.1148/radiol.14140754
36. Idilman IS, Aniktar H, Idilman R, Kabacam G, Savas B, Elhan A, et al. Hepatic steatosis: quantification by proton density fat fraction with MR imaging versus liver biopsy. *Radiology* 2013; **267**: 767–75. doi: https://doi.org/10.1148/radiol.13121360
37. Cunha GM, Thai TT, Hamilton G, Covarrubias Y, Schlein A, Middleton MS, et al. Accuracy of common proton density fat fraction thresholds for magnitude- and complex-based chemical shift-encoded MRI for assessing hepatic steatosis in patients with obesity. *Abdom Radiol* 2020; **45**: 661–71. doi: https://doi.org/10.1007/s00261-019-02350-3
38. Gu J, Liu S, Du S, Zhang Q, Xiao J, Dong Q, et al. Diagnostic value of MRI-PDFF for hepatic steatosis in patients with non-alcoholic fatty liver disease: a meta-analysis. *Eur Radiol* 2019; **29**: 3564–73. doi: https://doi.org/10.1007/s00330-019-06072-4
39. Bohte AE, van Werven JR, Bipat S, Stoker J. The diagnostic accuracy of US, CT, MRI and 1H-MRS for the evaluation of hepatic steatosis compared with liver biopsy: a meta-analysis. *Eur Radiol* 2011; **21**: 87–97. doi: https://doi.org/10.1007/s00330-010-1905-5
40. Zand KA, Shah A, Heba E, Wolfson T, Hamilton G, Lam J, et al. Accuracy of multiecho magnitude-based MRI (M-MRI) for estimation of hepatic proton density fat fraction (PDFF) in children. *J Magn Reson Imaging* 2015; **42**: 1223–32. doi: https://doi.org/10.1002/jmri.24888
41. Kang GH, Cruite I, Shiehmorteza M, Wolfson T, Gamst AC, Hamilton G, et al. Reproducibility of MRI-determined proton density fat fraction across two different Mr scanner platforms. *J Magn Reson Imaging* 2011; **34**: 928–34. doi: https://doi.org/10.1002/jmri.22701
42. Yokoo T, Serai SD, Pirasteh A, Bashir MR, Hamilton G, Hernando D, et al. Linearity, bias, and precision of hepatic proton density fat fraction measurements by using MR imaging: a meta-analysis. *Radiology* 2018; **286**: 486–98. doi: https://doi.org/10.1148/radiol.2017170550
43. Middleton MS, Heba ER, Hooker CA, Bashir MR, Fowler KJ, Sandrasegaran K, et al. Agreement between magnetic resonance imaging proton density fat fraction measurements and pathologist-assigned steatosis grades of liver biopsies from adults with nonalcoholic steatohepatitis. *Gastroenterology* 2017; **153**: 753–61. doi: https://doi.org/10.1053/j.gastro.2017.06.005
44. Stine JG, Munaganuru N, Barnard A, Wang JL, Kaulback K, Argo CK, et al. Change in MRI-PDFF and histologic response in patients with nonalcoholic steatohepatitis: a systematic review and meta-analysis. *Clin Gastroenterol Hepatol* 2020;31 Aug 2020. doi: https://doi.org/10.1016/j.cgh.2020.08.061
45. Wang K, Mamidipalli A, Retson T, Bahrami N, Hasenstab K, Blansit K, et al. Automated CT and MRI liver segmentation and biometry using a generalized Convolutional neural network. *Radiol Artif Intell* 2019; **1**: 180022. doi: https://doi.org/10.1148/ryai.2019180022
46. Dulai PS, Singh S, Patel J, Soni M, Prokop LJ, Younossi Z, et al. Increased risk of mortality by fibrosis stage in nonalcoholic fatty liver disease: systematic review and meta-analysis. *Hepatology* 2017; **65**: 1557–65. doi: https://doi.org/10.1002/hep.29085
47. Angulo P, Kleiner DE, Dam-Larsen S, Adams LA, Bjornsson ES, Charatcharoenwitthaya P, et al. Liver fibrosis, but no other histologic features, is associated with long-term outcomes of patients with nonalcoholic fatty liver disease. *Gastroenterology* 2015; **149**: 389–97. doi: https://doi.org/10.1053/j.gastro.2015.04.043
48. Petitclerc L, Sebastiani G, Gilbert G, Cloutier G, Tang A. Liver fibrosis: review of current imaging and MRI quantification techniques. *J Magn Reson Imaging* 2017; **45**: 1276–95. doi: https://doi.org/10.1002/jmri.25550
49. Park HJ, Lee SS, Park B, Yun J, Sung YS, Shim WH, et al. Radiomics analysis of gadoxetic acid-enhanced MRI for staging liver fibrosis. *Radiology* 2019; **290**: 380–7. doi: https://doi.org/10.1148/radiol.2018181197
50. Ni M, Wang L, Yu H, Wen X, Yang Y, Liu G, et al. Radiomics Approaches for Predicting Liver Fibrosis With Nonenhanced T 1 - Weighted Imaging: Comparison of Different Radiomics Models. *J Magn Reson Imaging* 2020; **16**. doi: https://doi.org/10.1002/jmri.27391
51. Idilman IS, Li J, Yin M, Venkatesh SK. Mr elastography of liver: current status and future perspectives. *Abdom Radiol* 2020; **45**: 1–19. doi: https://doi.org/10.1007/s00261-020-02656-7
52. Venkatesh SK, Yin M, Ehman RL. Magnetic resonance elastography of liver: technique, analysis, and clinical applications. *J Magn Reson Imaging* 2013; **37**: 544–55. doi: https://doi.org/10.1002/jmri.23731
53. Quantitative Imaging Biomarkers Alliance. Magnetic resonance elastography of the Liver: radiological society of North America. 2018. Available from: http://qibawiki.rsna.org/index.php/Profiles.
54. Dzyubak B, Venkatesh SK, Manduca A, Glaser KJ, Ehman RL. Automated liver elasticity calculation for Mr elastography. *J*

Magn Reson Imaging 2016; **43**: 1055–63. doi: https://doi.org/10.1002/jmri.25072
55. Horowitz JM, Venkatesh SK, Ehman RL, Jhaveri K, Kamath P, Ohliger MA, et al. Evaluation of hepatic fibrosis: a review from the Society of abdominal radiology disease focus panel. *Abdom Radiol* 2017; **42**: 2037–53. doi: https://doi.org/10.1007/s00261-017-1211-7
56. Kim BH, Lee JM, Lee YJ, Lee KB, Suh K-S, Han JK, et al. Mr elastography for noninvasive assessment of hepatic fibrosis: experience from a tertiary center in Asia. *J Magn Reson Imaging* 2011; **34**: 1110–6. doi: https://doi.org/10.1002/jmri.22723
57. Venkatesh SK, Wang G, Lim SG, Wee A. Magnetic resonance elastography for the detection and staging of liver fibrosis in chronic hepatitis B. *Eur Radiol* 2014; **24**: 70–8. doi: https://doi.org/10.1007/s00330-013-2978-8
58. Singh S, Venkatesh SK, Loomba R, Wang Z, Sirlin C, Chen J, et al. Magnetic resonance elastography for staging liver fibrosis in non-alcoholic fatty liver disease: a diagnostic accuracy systematic review and individual participant data pooled analysis. *Eur Radiol* 2016; **26**: 1431–40. doi: https://doi.org/10.1007/s00330-015-3949-z
59. Singh S, Venkatesh SK, Wang Z, Miller FH, Motosugi U, Low RN, et al. Diagnostic performance of magnetic resonance elastography in staging liver fibrosis: a systematic review and meta-analysis of individual participant data. *Clin Gastroenterol Hepatol* 2015; **13**: 440–51. doi: https://doi.org/10.1016/j.cgh.2014.09.046
60. Wang Q-B, Zhu H, Liu H-L, Zhang B. Performance of magnetic resonance elastography and diffusion-weighted imaging for the staging of hepatic fibrosis: a meta-analysis. *Hepatology* 2012; **56**: 239–47. doi: https://doi.org/10.1002/hep.25610
61. Guo Y, Parthasarathy S, Goyal P, McCarthy RJ, Larson AC, Miller FH. Magnetic resonance elastography and acoustic radiation force impulse for staging hepatic fibrosis: a meta-analysis. *Abdom Imaging* 2015; **40**: 818–34. doi: https://doi.org/10.1007/s00261-014-0137-6
62. Serai SD, Obuchowski NA, Venkatesh SK, Sirlin CB, Miller FH, Ashton E, et al. Repeatability of Mr elastography of liver: a meta-analysis. *Radiology* 2017; **285**: 92–100. doi: https://doi.org/10.1148/radiol.2017161398
63. Gidener T, Ahmed OT, Larson JJ, Mara KC, Therneau TM, Venkatesh SK, et al. Liver stiffness by magnetic resonance elastography predicts future cirrhosis, decompensation, and death in NAFLD. *Clin Gastroenterol Hepatol* 2020;30 Sep 2020. doi: https://doi.org/10.1016/j.cgh.2020.09.044
64. Idilman IS, Low HM, Bakhshi Z, Eaton J, Venkatesh SK. Comparison of liver stiffness measurement with MRE and liver and spleen volumetry for prediction of disease severity and hepatic decompensation in patients with primary sclerosing cholangitis. *Abdom Radiol* 2020; **45**: 701–9. doi: https://doi.org/10.1007/s00261-019-02387-4
65. Cho HJ, Kim B, Kim HJ, Huh J, Kim JK, Lee JH, et al. Liver stiffness measured by Mr elastography is a predictor of early HCC recurrence after treatment. *Eur Radiol* 2020; **30**: 1–11. doi: https://doi.org/10.1007/s00330-020-06792-y
66. Ajmera VH, Liu A, Singh S, Yachoa G, Ramey M, Bhargava M, et al. Clinical utility of an increase in magnetic resonance elastography in predicting fibrosis progression in nonalcoholic fatty liver disease. *Hepatology* 2020; **71**: 849–60. doi: https://doi.org/10.1002/hep.30974
67. Eaton JE, Sen A, Hoodeshenas S, Schleck CD, Harmsen WS, Gores GJ, et al. Changes in liver stiffness, measured by magnetic resonance elastography, associated with hepatic decompensation in patients with primary sclerosing cholangitis. *Clin Gastroenterol Hepatol* 2020; **18**: 1576–83. doi: https://doi.org/10.1016/j.cgh.2019.10.041
68. Navin PJ, Gidener T, Allen AM, Yin M, Takahashi N, Torbenson MS, et al. The role of magnetic resonance elastography in the diagnosis of noncirrhotic portal hypertension. *Clin Gastroenterol Hepatol* 2020; **18**: 3051-3053.e2. doi: https://doi.org/10.1016/j.cgh.2019.10.018
69. Kim DW, Kim SY, Yoon HM, Kim KW, Byun JH. Comparison of technical failure of Mr elastography for measuring liver stiffness between gradient-recalled echo and spin-echo echo-planar imaging: a systematic review and meta-analysis. *J Magn Reson Imaging* 2020; **51**: 1086–102. doi: https://doi.org/10.1002/jmri.26918
70. Morin CE, Dillman JR, Serai SD, Trout AT, Tkach JA, Wang H. Comparison of standard Breath-Held, Free-Breathing, and compressed sensing 2D gradient-recalled echo Mr elastography techniques for evaluating liver stiffness. *AJR Am J Roentgenol* 2018; **211**: W279–87. doi: https://doi.org/10.2214/AJR.18.19761
71. Delgado TI, Cunha GM, Hasenstab KA, et al. Agreement between MR elastography liver stiffness estimates obtained from fully automated convolutional neural network-based and manually drawn regions-of-interest in ESGAR 2019 book of Abstracts. *Insights Imaging* 2019; **10**(Suppl 2): 58.
72. Onur MR, Poyraz AK, Bozdag PG, Onder S, Aygun C. Diffusion weighted MRI in chronic viral hepatitis: correlation between ADC values and histopathological scores. *Insights Imaging* 2013; **4**: 339–45. doi: https://doi.org/10.1007/s13244-013-0252-x
73. Sandrasegaran K, Territo P, Elkady RM, Lin Y, Gasparis P, Borthakur G, et al. Does intravoxel incoherent motion reliably stage hepatic fibrosis, steatosis, and inflammation? *Abdom Radiol* 2018; **43**: 600–6. doi: https://doi.org/10.1007/s00261-017-1263-8
74. Yoon JH, Lee JM, Suh K-S, Lee K-W, Yi N-J, Lee KB, et al. Combined use of Mr fat quantification and MR elastography in living liver donors: can it reduce the need for preoperative liver biopsy? *Radiology* 2015; **276**: 453–64. doi: https://doi.org/10.1148/radiol.15140908
75. França M, Martí-Bonmatí L, Alberich-Bayarri Ángel, Oliveira P, Guimaraes S, Oliveira J, et al. Evaluation of fibrosis and inflammation in diffuse liver diseases using intravoxel incoherent motion diffusion-weighted MR imaging. *Abdom Radiol* 2017; **42**: 468–77. doi: https://doi.org/10.1007/s00261-016-0899-0
76. Leitão HS, Doblas S, Garteiser P, d'Assignies G, Paradis V, Mouri F, et al. Hepatic fibrosis, inflammation, and steatosis: influence on the Mr viscoelastic and diffusion parameters in patients with chronic liver disease. *Radiology* 2017; **283**: 98–107. doi: https://doi.org/10.1148/radiol.2016151570
77. Tosun M, Onal T, Uslu H, Alparslan B, Çetin Akhan S. Intravoxel incoherent motion imaging for diagnosing and staging the liver fibrosis and inflammation. *Abdom Radiol* 2020; **45**: 15–23. doi: https://doi.org/10.1007/s00261-019-02300-z
78. Lefebvre T, Hébert M, Bilodeau L, Sebastiani G, Cerny M, Olivié D, et al. Intravoxel incoherent motion diffusion-weighted MRI for the characterization of inflammation in chronic liver disease. *Eur Radiol* 2021; **31**: 1347–58. doi: https://doi.org/10.1007/s00330-020-07203-y
79. Chen B-B, Hsu C-Y, Yu C-W, Kao J-H, Lee H-S, Liang P-C, et al. Hepatic necro-inflammation and elevated liver enzymes: evaluation with MRI perfusion imaging with gadoxetic acid in chronic hepatitis patients. *Clin Radiol* 2014; **69**: 473–80. doi: https://doi.org/10.1016/j.crad.2013.12.003
80. Hoad CL, Palaniyappan N, Kaye P, Chernova Y, James MW, Costigan C, et al. A study of T_1 relaxation time as a measure of liver fibrosis and the influence of confounding histological factors. *NMR Biomed* 2015; **28**: 706–14. doi: https://doi.org/10.1002/nbm.3299

81. Hueper K, Lang H, Hartleben B, Gutberlet M, Derlin T, Getzin T, et al. Assessment of liver ischemia reperfusion injury in mice using hepatic T_2 mapping: Comparison with histopathology. *J Magn Reson Imaging* 2018; **48**: 1586–94. doi: https://doi.org/10.1002/jmri.26057
82. Bradley C, Scott RA, Cox E, Palaniyappan N, Thomson BJ, Ryder SD, et al. Short-term changes observed in multiparametric liver MRI following therapy with direct-acting antivirals in chronic hepatitis C virus patients. *Eur Radiol* 2019; **29**: 3100–7. doi: https://doi.org/10.1007/s00330-018-5788-1
83. Pavlides M, Banerjee R, Tunnicliffe EM, Kelly C, Collier J, Wang LM, et al. Multiparametric magnetic resonance imaging for the assessment of non-alcoholic fatty liver disease severity. *Liver Int* 2017; **37**: 1065–73. doi: https://doi.org/10.1111/liv.13284
84. Song J, Yu X, Song W, Guo D, Li C, Liu H, et al. MRI-based Radiomics models developed with features of the whole liver and right liver lobe: assessment of hepatic inflammatory activity in chronic hepatic disease. *J Magn Reson Imaging* 2020; **52**: 1668–78. doi: https://doi.org/10.1002/jmri.27197
85. Yin M, Glaser KJ, Manduca A, Mounajjed T, Malhi H, Simonetto DA, et al. Distinguishing between hepatic inflammation and fibrosis with Mr elastography. *Radiology* 2017; **284**: 694–705. doi: https://doi.org/10.1148/radiol.2017160622
86. Allen AM, Shah VH, Therneau TM, Venkatesh SK, Mounajjed T, Larson JJ, et al. The role of three-dimensional magnetic resonance elastography in the diagnosis of nonalcoholic steatohepatitis in obese patients undergoing bariatric surgery. *Hepatology* 2020; **71**: 510–21. doi: https://doi.org/10.1002/hep.30483
87. Allen AM, Shah VH, Therneau TM, Venkatesh SK, Mounajjed T, Larson JJ, et al. Multiparametric magnetic resonance elastography improves the detection of NASH regression following bariatric surgery. *Hepatol Commun* 2020; **4**: 185–92. doi: https://doi.org/10.1002/hep4.1446
88. Dam-Larsen S, Franzmann M, Andersen IB, Christoffersen P, Jensen LB, Sørensen TIA, et al. Long term prognosis of fatty liver: risk of chronic liver disease and death. *Gut* 2004; **53**: 750–5. doi: https://doi.org/10.1136/gut.2003.019984
89. Parente DB, Paiva FF, Oliveira Neto JA, Machado-Silva L, Figueiredo FAF, Lanzoni V, et al. Intravoxel incoherent motion diffusion weighted MR imaging at 3.0 T: assessment of steatohepatitis and fibrosis compared with liver biopsy in type 2 diabetic patients. *PLoS One* 2015; **10**: e0125653. doi: https://doi.org/10.1371/journal.pone.0125653
90. Murphy P, Hooker J, Ang B, Wolfson T, Gamst A, Bydder M, et al. Associations between histologic features of nonalcoholic fatty liver disease (NAFLD) and quantitative diffusion-weighted MRI measurements in adults. *J Magn Reson Imaging* 2015; **41**: 1629–38. doi: https://doi.org/10.1002/jmri.24755
91. Yin Z, Murphy MC, Li J, Glaser KJ, Mauer AS, Mounajjed T, et al. Prediction of nonalcoholic fatty liver disease (NAFLD) activity score (NAS) with multiparametric hepatic magnetic resonance imaging and elastography. *Eur Radiol* 2019; **29**: 5823–31. doi: https://doi.org/10.1007/s00330-019-06076-0
92. Srivastava A, Jong S, Gola A, Gailer R, Morgan S, Sennett K, et al. Cost-comparison analysis of FIB-4, ELF and fibroscan in community pathways for non-alcoholic fatty liver disease. *BMC Gastroenterol* 2019; **19**: 122. doi: https://doi.org/10.1186/s12876-019-1039-4
93. Crossan C, Tsochatzis EA, Longworth L, Gurusamy K, Davidson B, Rodríguez-Perálvarez M, et al. Cost-effectiveness of non-invasive methods for assessment and monitoring of liver fibrosis and cirrhosis in patients with chronic liver disease: systematic review and economic evaluation. *Health Technol Assess* 2015; **19**: 1–410. doi: https://doi.org/10.3310/hta19090
94. Crossan C, Majumdar A, Srivastava A, Thorburn D, Rosenberg W, Pinzani M, et al. Referral pathways for patients with NAFLD based on non-invasive fibrosis tests: diagnostic accuracy and cost analysis. *Liver Int* 2019; **39**: 2052–60. doi: https://doi.org/10.1111/liv.14198
95. Xiao G, Zhu S, Xiao X, Yan L, Yang J, Wu G. Comparison of laboratory tests, ultrasound, or magnetic resonance elastography to detect fibrosis in patients with nonalcoholic fatty liver disease: a meta-analysis. *Hepatology* 2017; **66**: 1486–501. doi: https://doi.org/10.1002/hep.29302